JOURNAL OF MAGNETIC RESONANCE **134,** 7–16 (1998)
ARTICLE NO. MN981509

The Complete Homogeneous Master Equation for a Heteronuclear Two-Spin System in the Basis of Cartesian Product Operators

Peter Allard,[1] Magnus Helgstrand, and Torleif Härd

Department of Biotechnology, The Royal Institute of Technology, Center for Structural Biochemistry, Novum, Huddinge, S-141 57, Sweden

Received December 16, 1997; revised April 27, 1998

The complete homogeneous form of the quantum mechanical master equation for a heteronuclear two-spin system is presented in the basis of Cartesian product operators. The homogeneous master equation is useful since it allows fast, single-step computation of the density operator during pulse sequences, without neglecting relaxation effects. The homogeneous master equation is also a prerequisite for an expansion of the average Hamiltonian theory to include relaxation, thus forming average Liouvillian theory. The coherences of the two-spin system are assumed to be relaxed both by mutual dipole–dipole interaction and by chemical shift anisotropy interaction with the static magnetic field. The cross-correlation between dipole–dipole and chemical shift anisotropy relaxation mechanisms is also considered. To illustrate the applicability of the developed formalism we simulate the overall transfer efficiency of three different inverse detection $^{1}H–^{15}N$ correlation experiments with parameters corresponding to a large protein.

Key Words: **homogeneous master equation; NMR simulations; average Liouvillian theory; coherence transfer; heteronuclear two-spin system.**

INTRODUCTION

The ordinary quantum mechanical master equation describing the evolution of the density operator including relaxation, the Liouville–von Neumann equation, has the mathematical form of an inhomogeneous differential equation (*1*, *2*). The fact that it is inhomogeneous obviously complicates its use for obtaining analytical and numerical solutions to NMR-related problems. One possible approach to the problem is to ignore relaxation altogether. Without relaxation the Liouville–von Neumann equation is homogeneous. A second, more common approach is to ignore relaxation during RF pulses and to include relaxation only during periods of free precession. This simplifies the calculations since the spin Hamiltonian commutes with the equilibrium density operator in the absence of an RF field, and a simple substitution makes the master equation homogeneous (*3*). Obviously, neither of these methods represents a complete solution to the problem.

It has been shown, however, that the Liouville–von Neumann equation can be rewritten in a homogeneous form without introducing any approximations (*4*). The practical details regarding the implementation have been sorted out both in the basis of level shift operators (*4*, *5*), and in the basis of Cartesian product operators (*6–8*). The homogeneous master equation (HME) is in our opinion easier to understand when expressed in the basis of Cartesian product operators. The previous papers dealing with the HME in the basis of Cartesian product operators for a heteronuclear spin system (*6*, *7*) only give the solution for the limited part of Liouville space related to the extended Solomon equations (*9*). We feel that the HME for the complete Liouville space is useful, especially in the simulations of pulse sequences. We have previously presented the full theory for a homonuclear spin system and from the full theory derived the homogeneous form of the Bloch–Solomon equations (*8*).

Average Hamiltonian theory has been used in the development of composite pulse sequences in which a specific Hamiltonian is required during a certain time interval (*2*). The homogeneous master equation makes it possible to formulate an average Hamiltonian theory in combination with an average relaxation superoperator, which is named average Liouvillian theory (*6*, *7*). Average Liouvillian theory will be useful in the development of pulse sequences that modifies the effective relaxation superoperator, i.e., if certain relaxation pathways are required to be open while others are required to be closed during a time interval.

In order to illustrate the applicability of the complete HME we have simulated the transfer efficiency for three different types of inverse detection $^{1}H–^{15}N$ correlation experiments. The experiments are an ordinary phase cycled HSQC experiment (*10*), a sensitivity enhanced gradient selected HSQC experiment (*11*), and a heteronuclear cross-polarization (CP) (*12*) based experiment. Molecular parameters assumed in the simulations correspond to those of a macromolecule. Transfer efficiencies as a function of offset chemical shifts are presented

[1] To whom correspondence should be addressed. Fax: 46-8-608-92-90. E-mail: peter@csb.ki.se

1090-7807/98 $25.00

for all pulse sequences. Relaxation is included in all parts of the simulations.

THEORY

Introduction

We will calculate the homogeneous form of the quantum mechanical master equation (*4*) for a scalar-coupled heteronuclear two-spin system in the basis of Cartesian product operators (*6, 7*).

The spin Hamiltonian for a scalar-coupled heteronuclear two-spin system in the presence of two different RF fields can be written using the Cartesian product operators (*13*) as

$$H_{0,RF}(t) = H_0 + H_{RF}(t) \quad [1]$$

with

$$H_0 = \omega_I I_z + \omega_S S_z + \pi J 2 I_z S_z \quad [2]$$

and

$$\begin{aligned} H_{RF}(t) = &-B_{I1}\gamma_I\{I_x\cos(\omega_{I,RF}t + \phi_I) + I_y\sin(\omega_{I,RF}t + \phi_I)\} \\ &-B_{S1}\gamma_S\{S_x\cos(\omega_{S,RF}t + \phi_S) + S_y\sin(\omega_{S,RF}t + \phi_S)\}, \end{aligned} \quad [3]$$

where ω_I and ω_S are the angular Larmor frequencies of spin I and S; J is the scalar coupling constant between the two spins in hertz; $\omega_{I,RF}$ and $\omega_{S,RF}$ are the two angular RF field frequencies; and B_{I1}, B_{S1}, ϕ_I, and ϕ_S are the strengths and phases of the two applied RF fields. The magnetogyric ratios for the two spins are denoted γ_I and γ_S.

It is advisable to render the spin Hamiltonian time-independent by a transformation into a doubly rotating frame rotating with the RF frequencies $\omega_{I,RF}$ and $\omega_{S,RF}$ about the z axis, using

$$\begin{aligned} H = &\exp[i\omega_{S,RF}S_z t]\exp[i\omega_{I,RF}I_z t]H_{0,RF}(t)\exp[-i\omega_{I,RF}I_z t] \\ &\times \exp[-i\omega_{S,RF}S_z t] - \omega_{I,RF}I_z - \omega_{S,RF}S_z. \end{aligned} \quad [4]$$

The time-independent spin Hamiltonian, H, for a scalar-coupled heteronuclear two-spin system in the doubly rotating frame can thus be written using the Cartesian product operators as

$$\begin{aligned} H = &\Omega_I I_z + \Omega_S S_z + \pi J 2 I_z S_z + \omega_{Ix} I_x \\ &+ \omega_{Sx} S_x + \omega_{Iy} I_y + \omega_{Sy} S_y \end{aligned} \quad [5]$$

with

$$\begin{aligned} \Omega_I &= \omega_I - \omega_{I,RF} \\ \Omega_S &= \omega_S - \omega_{S,RF} \\ \omega_{Ix} &= -\gamma_I B_{I1}\cos(\phi_I) \\ \omega_{Sx} &= -\gamma_S B_{S1}\cos(\phi_S) \\ \omega_{Iy} &= -\gamma_I B_{I1}\sin(\phi_I) \\ \omega_{Sy} &= -\gamma_S B_{S1}\sin(\phi_S), \end{aligned} \quad [6]$$

where Ω_I and Ω_S are the chemical shift offset frequencies in rad/s; and ω_{Ix}, ω_{Sx}, ω_{Iy} and ω_{Sy} are the RF magnetic field components at the two frequencies along the x and y axes in rad/s. The doubly rotating frame is assumed in all calculations in this paper.

The ordinary quantum mechanical master equation (*1, 2*), i.e., the Liouville–von Neumann equation for the evolution of the density operator σ in the presence of relaxation, has the form

$$\frac{d}{dt}\sigma = -i\hat{\hat{H}}\sigma - \hat{\hat{\Gamma}}(\sigma - \sigma_0) \quad [7]$$

with

$$\hat{\hat{H}}\sigma = [H, \sigma], \quad [8]$$

where $\hat{\hat{H}}$ is the commutator superoperator for the coherent spin–spin and spin–field interactions and $\hat{\hat{\Gamma}}$ is the relaxation superoperator that accounts for the relaxation of the density operator, σ, to equilibrium, σ_0. Double carets denote superoperators. The static equilibrium density operator is calculated according to

$$\sigma_0 = \frac{\exp[-\hbar H_0/kT]}{\mathrm{Tr}\{\exp[-\hbar H_0/kT]\}}, \quad [9]$$

where H_0 is defined in Eq. [2]; $\hbar$ is Planck's constant divided by 2π; k is Boltzmann's constant; and T is the absolute temperature in kelvins. The equilibrium density operator in the doubly rotating frame is the same as the static equilibrium density operator since it is invariant to rotations about the z axis.

It has been shown that the relaxation superoperator $\hat{\hat{\Gamma}}$ can be replaced by an improved relaxation superoperator, $\hat{\hat{\Gamma}}_{imp}$, transforming the inhomogeneous master equation into a homogeneous form (*4*),

$$\frac{d}{dt}\sigma = -(i\hat{\hat{H}} + \hat{\hat{\Gamma}}_{imp})\sigma. \quad [10]$$

This is the equation we want to derive for a heteronuclear two-spin system. The improved relaxation operator is adjusted for the thermal polarization by the surrounding lattice (*6, 7*).

It is convenient to use an operator basis set that includes the

unity operator E, since in this case the thermal correction can be performed using the otherwise empty column in the relaxation matrix corresponding to this operator (*6, 7*). This new column is calculated by multiplying the relaxation matrix $\hat{\Gamma}$ with the vector corresponding to the equilibrium density operator σ_0.

The Coherent Term

We will use the Cartesian product operators as an operator basis set for our calculations. For a two-spin system the 16 Cartesian product operators (*13*) are

$$\begin{aligned} &B^{2spin} = E/2, \\ &I_x,\ I_y,\ I_z,\ S_x,\ S_y,\ S_z, \\ &2I_xS_x,\ 2I_xS_y,\ 2I_xS_z, \\ &2I_yS_x,\ 2I_yS_y,\ 2I_yS_z, \\ &2I_zS_x,\ 2I_zS_y,\ 2I_zS_z. \end{aligned} \qquad [11]$$

The coherent part of the master equation in the basis of Cartesian product operators can be calculated directly from the basis operators in Eq. [11] and the rotating frame spin Hamiltonian in Eq. [5] using commutator relationships according to (*2*)

$$\begin{aligned} H_{rs} &= \langle B_r^{2spin}|\hat{\hat{H}}|B_s^{2spin}\rangle = \langle B_r^{2spin}|[H,\ B_s^{2spin}]\rangle \\ &= \langle B_r^{2spin}|HB_s^{2spin} - B_s^{2spin}H\rangle, \end{aligned} \qquad [12]$$

where r and s denote the two Cartesian product operators in the basis set for which a matrix element is calculated. It should be noted that this equation does not contain bras and kets in the usual Dirac state space of quantum mechanics, but rather superbras and superkets in a larger vector space named superspace (*14, 4*). The matrix elements calculated are included in the matrix of Eq. [19], which is to be presented later.

The Relaxation Term

When calculating the relaxation term in the master equation we assume that the two spins are dipole–dipole (DD) coupled and experience relaxation due to this coupling. We also assume that one of the spins, spin S, experiences relaxation due to chemical-shift anisotropy (CSA) and that the shielding tensor is axially symmetric. The spin I is also assumed to be relaxed by DD interactions with spins other than spin S. The possibility of cross-correlation between DD and CSA relaxation (*15, 16*) is finally also taken into account.

The elements of the relaxation matrix are calculated using Redfield theory with the secular and other well-known approximations (*1, 17*). The relaxation superoperator is in principle time-dependent since the eigenstates of the spin system are affected by the modulation induced by the external RF field. It is however reasonable to assume that $\omega_e\tau_c \ll 1$, where ω_e is the angular nuclear spin precession rate about the effective field and τ_c is the correlation time of the interactions responsible for relaxation. It can be shown that using this approximation the relaxation behavior is the same as in the absence of the RF field, but in a frame tilted relative to the static magnetic field (*18, 19*). The elements of the Redfield relaxation matrix in the basis of Cartesian product operators can then be calculated using Wigner 3-J symbols according to (*20, 21*)

$$\begin{aligned} \Gamma_{rs} = \frac{5}{3}\sum_{n,m} A_nA_m \sum_{q=-2,\mu=-1}^{q=2,\mu=1} \begin{bmatrix} 1 & 1 & 2 \\ \mu & q-\mu & -q \end{bmatrix}^2 \\ \times J^{nm}(\mu\omega_L^n + (q-\mu)\omega_K^n) \\ \times \mathrm{Tr}\{[L_\mu^m K_{q-\mu}^m,\ B_r^{2spin}]^\dagger [L_\mu^n K_{q-\mu}^n,\ B_s^{2spin}]\}, \end{aligned} \qquad [13]$$

where † denotes the adjoint and in which K and L are either the spherical spin operators for the two interacting spins in the case of DD relaxation or the spherical spin operator of the nucleus with anisotropy of shielding and the components of a unit vector oriented along the static external magnetic field in the case of CSA relaxation. The factor A_n is the strength of relaxation mechanism n, and $J(\omega)$ is the auto- or cross-correlation spectral density at the angular frequency ω. The indices n and m run over the different mechanisms involved in the relaxation, in this case DD and CSA. If n equals m, the autocorrelation relaxation rate of a particular mechanism is calculated, whereas if n is not equal to m, the cross-correlation relaxation rate between two mechanisms is calculated. The indices r and s denote the two Cartesian product operators in the basis set between which the relaxation rate is calculated. If r equals s, the autorelaxation rate of a particular basis operator is calculated, whereas if r is not equal to s, the cross-relaxation rate between two basis operators is calculated. The strengths of the DD and the CSA relaxation mechanisms are given by

$$A_d = 3\left(\frac{\mu_0}{4\pi}\right)\left(\frac{\hbar\gamma_I\gamma_S}{r_{IS}^3}\right) \qquad [14]$$

and

$$A_c = -(\sigma_\parallel - \sigma_\perp)\gamma_S B_0, \qquad [15]$$

respectively, where μ_0 is the permeability of vacuum; r_{IS} is the distance between spins I and S; $\sigma_\parallel$ and $\sigma_\perp$ are the shielding constants for the parallel and perpendicular directions an axially symmetric shielding tensor, respectively; and B_0 is the static magnetic field strength of the magnet.

The dynamic properties of vectors in the molecule in which the spins reside can be described by a model. The model can then be used in order to derive an analytical spectral density function, $J(\omega)$. The relaxation rates described by Eq. [13] are functions of the spectral density function at certain angular frequencies. In our simulations we will consider the model for dynamics derived using the Lipari–Szabo approach (*22*, *23*). The analytical spectral density function for this model is

$$J(\omega) = \frac{2}{5}\left[\frac{S^2\tau_m}{1 + (\omega\tau_m)^2} + \frac{(1 - S^2)\tau_i}{1 + (\omega\tau_i)^2}\right] \quad [16]$$

with

$$\frac{1}{\tau_i} = \frac{1}{\tau_m} + \frac{1}{\tau_e}, \quad [17]$$

where τ_m is the overall rotational correlation time for a molecule; τ_e is the correlation time of internal motions; and S^2 an order parameter that describes the balance between contributions to relaxation due to overall rotation and internal motion. The assumptions behind the Lipari–Szabo model are that the overall rotation is isotropic and that the two motions are statistically independent.

There are three different spectral density functions to be considered, $J^{dd}(\omega)$, $J^{cc}(\omega)$, and $J^{cd}(\omega)$, corresponding to DD autocorrelation, CSA autocorrelation, and DD–CSA cross-correlation, respectively. If isotropic rotational diffusion of a rigid body is assumed, there is a simple relation between the different spectral densities (*24*)

$$J(\omega) = J^{dd}(\omega) = J^{cc}(\omega) = J^{cd}(\omega)/\tfrac{1}{2}\,(3\cos^2(\varphi) - 1), \quad [18]$$

where φ is the angle between the unique axis of the CSA tensor and the internuclear vector r_{IS}. This equation is not rigorously correct in the presence of internal motion, i.e., if $S^2 < 1$, but it is a good approximation if φ is small (*24*).

The relaxation matrix elements calculated from Eq. [13] and the relations between spectral densities from Eq. [18] are included in the matrix of Eq. [19].

The Homogeneous Master Equation

We now present the explicit matrix representation of Eq. [10] by adding up the coherent terms from Eq. [12] and the relaxation terms from Eq. [13]. The matrix must also be corrected for thermal polarization. The first column in the matrix corresponds to the unity operator $E/2$. The thermal correction vector for equilibrium magnetization with the elements Θ_I, Θ_S, and Θ_{IS} is inserted at this position. The vector is calculated as described before by multiplying $\hat{\hat{\Gamma}}$ with σ_0, followed by multiplication by the factor -2 in order to account for the minus sign in front of the matrix and the fact that we use the operator $E/2$ in our basis set and not E. The result is

$$\frac{d}{dt}\begin{bmatrix} E/2 \\ I_x \\ I_y \\ I_z \\ S_x \\ S_y \\ S_z \\ 2I_xS_z \\ 2I_yS_z \\ 2I_zS_x \\ 2I_zS_y \\ 2I_xS_x \\ 2I_xS_y \\ 2I_yS_x \\ 2I_yS_y \\ 2I_zS_z \end{bmatrix} = -\begin{bmatrix} 0 & 0 & 0 & 0 & 0 & 0 & 0 & 0 & 0 & 0 & 0 & 0 & 0 & 0 & 0 & 0 \\ 0 & \lambda_I & \Omega_I & -\omega_{Iy} & 0 & 0 & 0 & 0 & \pi J & 0 & 0 & 0 & 0 & 0 & 0 & 0 \\ 0 & -\Omega_I & \lambda_I & \omega_{Ix} & 0 & 0 & 0 & -\pi J & 0 & 0 & 0 & 0 & 0 & 0 & 0 & 0 \\ -2\Theta_I & \omega_{Iy} & -\omega_{Ix} & \rho_I & 0 & 0 & \sigma & 0 & 0 & 0 & 0 & 0 & 0 & 0 & 0 & 0 \\ 0 & 0 & 0 & 0 & \lambda_S & \Omega_S & -\omega_{Sy} & 0 & 0 & \eta_S & \pi J & 0 & 0 & 0 & 0 & 0 \\ 0 & 0 & 0 & 0 & -\Omega_S & \lambda_S & \omega_{Sx} & 0 & 0 & -\pi J & \eta_S & 0 & 0 & 0 & 0 & 0 \\ -2\Theta_S & 0 & 0 & \sigma & \omega_{Sy} & -\omega_{Sx} & \rho_S & 0 & 0 & 0 & 0 & 0 & 0 & 0 & 0 & \delta_S \\ 0 & 0 & \pi J & 0 & 0 & 0 & 0 & \rho_I^a & \Omega_I & 0 & 0 & \omega_{Sy} & -\omega_{Sx} & 0 & 0 & -\omega_{Iy} \\ 0 & -\pi J & 0 & 0 & 0 & 0 & 0 & -\Omega_I & \rho_I^a & 0 & 0 & 0 & 0 & \omega_{Sy} & -\omega_{Sx} & \omega_{Ix} \\ 0 & 0 & 0 & 0 & \eta_S & \pi J & 0 & 0 & 0 & \rho_S^a & \Omega_S & \omega_{Iy} & 0 & -\omega_{Ix} & 0 & -\omega_{Sy} \\ 0 & 0 & 0 & 0 & -\pi J & \eta_S & 0 & 0 & 0 & -\Omega_S & \rho_S^a & 0 & \omega_{Iy} & 0 & -\omega_{Ix} & \omega_{Sx} \\ 0 & 0 & 0 & 0 & 0 & 0 & 0 & -\omega_{Sy} & 0 & -\omega_{Iy} & 0 & \lambda^{mq} & \Omega_S & \Omega_I & -\mu^{mq} & 0 \\ 0 & 0 & 0 & 0 & 0 & 0 & 0 & \omega_{Sx} & 0 & 0 & -\omega_{Iy} & -\Omega_S & \lambda^{mq} & \mu^{mq} & \Omega_I & 0 \\ 0 & 0 & 0 & 0 & 0 & 0 & 0 & 0 & -\omega_{Sy} & \omega_{Ix} & 0 & -\Omega_I & \mu^{mq} & \lambda^{mq} & \Omega_S & 0 \\ 0 & 0 & 0 & 0 & 0 & 0 & 0 & 0 & \omega_{Sx} & 0 & \omega_{Ix} & -\mu^{mq} & -\Omega_I & -\Omega_S & \lambda^{mq} & 0 \\ -2\Theta_{IS} & 0 & 0 & 0 & 0 & 0 & \delta_S & \omega_{Iy} & -\omega_{Ix} & \omega_{Sy} & -\omega_{Sx} & 0 & 0 & 0 & 0 & \rho_{IS}^{2sp} \end{bmatrix}\begin{bmatrix} E/2 \\ I_x \\ I_y \\ I_z \\ S_x \\ S_y \\ S_z \\ 2I_xS_z \\ 2I_yS_z \\ 2I_zS_x \\ 2I_zS_y \\ 2I_xS_x \\ 2I_xS_y \\ 2I_yS_x \\ 2I_yS_y \\ 2I_zS_z \end{bmatrix}, \quad [19]$$

with

$$\Theta_I = \rho_I M_{I0} + \sigma M_{S0} \quad [20]$$

$$\Theta_S = \sigma M_{I0} + \rho_S M_{S0} \quad [21]$$

$$\Theta_{IS} = \delta_S M_{S0} \quad [22]$$

and

$$\lambda_S = \frac{1}{36} A_d^2 \Big[2J(0) + \frac{3}{2} J(\omega_S) + \frac{1}{2} J(\omega_I - \omega_S) + 3J(\omega_I) + 3J(\omega_I + \omega_S) \Big] + \frac{1}{3} A_c^2 \Big[\frac{2}{3} J(0) + \frac{1}{2} J(\omega_S) \Big] \quad [23]$$

$$\lambda_I = \frac{1}{36} A_d^2 \Big[2J(0) + 3J(\omega_S) + \frac{1}{2} J(\omega_I - \omega_S) + \frac{3}{2} J(\omega_I) + 3J(\omega_I + \omega_S) \Big] + \lambda_H \quad [24]$$

$$\rho_S = \frac{1}{36} A_d^2 [3J(\omega_S) + J(\omega_I - \omega_S) + 6J(\omega_I + \omega_S)] + \frac{1}{3} A_c^2 [J(\omega_S)] \quad [25]$$

$$\rho_I = \frac{1}{36} A_d^2 [J(\omega_I - \omega_S) + 3J(\omega_I) + 6J(\omega_I + \omega_S)] + \rho_H \quad [26]$$

$$\rho_S^a = \frac{1}{36} A_d^2 \Big[2J(0) + \frac{3}{2} J(\omega_S) + \frac{1}{2} J(\omega_I - \omega_S) + 3J(\omega_I + \omega_S) \Big] + \frac{1}{3} A_c^2 \Big[\frac{2}{3} J(0) + \frac{1}{2} J(\omega_S) \Big] + \rho_H \quad [27]$$

$$\rho_I^a = \frac{1}{36} A_d^2 \Big[2J(0) + \frac{1}{2} J(\omega_I - \omega_S) + \frac{3}{2} J(\omega_I) + 3J(\omega_I + \omega_S) \Big] + \frac{1}{3} A_c^2 [J(\omega_S)] + \lambda_H \quad [28]$$

$$\lambda^{mq} = \frac{1}{36} A_d^2 \Big[\frac{3}{2} J(\omega_S) + \frac{1}{2} J(\omega_I - \omega_S) + \frac{3}{2} J(\omega_I) + 3J(\omega_I + \omega_S) \Big] + \frac{1}{3} A_c^2 \Big[\frac{2}{3} J(0) + \frac{1}{2} J(\omega_S) \Big] + \lambda_H \quad [29]$$

$$\rho_{IS}^{2sp} = \frac{1}{36} A_d^2 [3J(\omega_S) + 3J(\omega_I)] + \frac{1}{3} A_c^2 [J(\omega_S)] + \rho_H \quad [30]$$

$$\sigma = \frac{1}{36} A_d^2 [-J(\omega_I - \omega_S) + 6J(\omega_I + \omega_S)] \quad [31]$$

$$\mu^{mq} = \frac{1}{36} A_d^2 \Big[-\frac{1}{2} J(\omega_I - \omega_S) + 3J(\omega_I + \omega_S) \Big] \quad [32]$$

$$\delta_S = \frac{1}{3} A_d A_c \frac{1}{2} [3 \cos^2(\varphi) - 1][J(\omega_S)] \quad [33]$$

$$\eta_S = \frac{1}{3} A_d A_c \frac{1}{2} [3 \cos^2(\varphi) - 1] \Big[\frac{2}{3} J(0) + \frac{1}{2} J(\omega_S) \Big], \quad [34]$$

where M_{I0} and M_{S0} are the equilibrium magnetizations of spin I and S, respectively; λ is the relaxation rate for transverse in-phase magnetization; ρ is the relaxation rate for longitudinal magnetization; ρ_I^a is the relaxation rate for transverse spin I magnetization that is antiphase with respect to spin S; λ^{mq} represents relaxation rates for multiple-quantum coherences; ρ^{2sp} is the relaxation rate for longitudinal two-spin order; σ is the longitudinal cross-relaxation rate; μ^{mq} is a cross-relaxation rate between multiple-quantum coherence components; δ_S is the longitudinal cross-correlation relaxation rate; and η_S is the transverse cross-correlation relaxation rate.

We have also assumed that spin I can be relaxed due to DD relaxation by spins other than spin S in the neighborhood of I. In order to take this into account we have added λ_H as additional transverse relaxation in Eqs. [24], [28], [29] and ρ_H as additional longitudinal relaxation in Eqs. [26], [27], and [30] (*21*).

It should be noted that the approximations introduced by Eq. [18] are not crucial in the derivation of Eq. [19]. Equation [19] can easily be made completely general with respect to any differences between, e.g., $J^{dd}(\omega)$ and $J^{cc}(\omega)$ by making appropriate substitutions in Eqs. [23]–[34].

The Solution to the Homogeneous Master Equation

The solution to the homogeneous master equation, Eq. [19], is

$$\sigma(t_1 + \Delta t) = \exp[-\hat{\hat{P}}\Delta t]\sigma(t = t_1), \quad [35]$$

where the relaxation Liouvillian $\hat{\hat{P}}$ is the matrix in Eq. [19] and $\exp[-\hat{P}\Delta t]$ is a superoperator relaxation propagator (*5*). The expectation value for an observable corresponding to the operator Obs is calculated using

$$\langle \text{Obs} \rangle = \langle \text{Obs}^\dagger | \sigma(t) \rangle. \quad [36]$$

Observable x and y magnetization correspond to the operators $\text{Obs} = I_x + S_x$ and $\text{Obs} = I_y + S_y$, respectively.

The effective relaxation Liouvillian $\hat{\hat{P}}_{eff}$ over a discrete number of steps, n, with their respective Liouvillians, $\hat{\hat{P}}_n$, and time periods, Δt_n, is defined by

$$\exp[-\hat{\hat{P}}_{eff} t_{tot}] = \exp[-\hat{\hat{P}}_n \Delta t_n] \cdots \exp[-\hat{\hat{P}}_2 \Delta t_2] \exp[-\hat{\hat{P}}_1 \Delta t_1], \quad [37]$$

where $t_{tot} = \sum_{i=1}^{n} \Delta t_i$ is the total time for the pulse sequence. The effective relaxation Liouvillian is calculated according to

$$\hat{\hat{P}}_{eff} = -\frac{1}{t_{tot}} \ln\{\exp[-\hat{\hat{P}}_n \Delta t_n] \cdots \exp[-\hat{\hat{P}}_2 \Delta t_2] \exp[-\hat{\hat{P}}_1 \Delta t_1]\}. \quad [38]$$

SIMULATIONS

Implementation

The simulations were performed using Matlab software version 5.1 on a 300 MHz Pentium 2 computer with Windows NT 4.0 as operating system. The relaxation rates were calculated using Eqs. [14], [15], [23]–[34], and [39] and [40] (not yet shown) with spectral densities from Eqs. [16]–[18]. The relaxation rates and the thermal correction from Eqs. [20]–[22] were inserted in the matrix of Eq. [19] together with relevant chemical shifts, scalar coupling, and RF fields. The time evolution of the density operator for different steps in the pulse sequences was evaluated with Eq. [35] using Matlab routines for calculating the exponent of a matrix. The observable x or y magnetization is identified as a single element in the calculated density operator σ and can be extracted with a scalar product according to Eq. [36].

Application to ^{1}H–^{15}N Correlation Experiments

To illustrate the applicability of the developed formalism we have simulated coherence transfer efficiencies for some common ^{1}H–^{15}N correlation experiments on a typical medium sized protein. The pulse sequences are presented in Figs. 1A–1C. Sequence (A) is an ordinary phase cycled HSQC experiment (*10*), sequence (B) is a sensitivity enhanced, phase modulated, gradient selected HSQC experiment (*11*), and sequence (C) is a heteronuclear cross-polarization (CP) based experiment (*12*). In Fig. 2 the simulated transfer efficiencies as a function of offset frequencies are presented for the pulse sequences presented in Fig. 1. Transfer efficiency in this case means the fraction of equilibrium ^{1}H magnetization that follows the desired coherence transfer pathways and can be detected as in-phase transverse x or y magnetization during acquisition.

We have used the following parameters in order to describe the two-spin system. The spins I and S are assigned to ^{1}H and ^{15}N nuclei, e.g., in a protein backbone amide. The one-bond scalar coupling constant is 92 Hz. The molecular dynamics are described by the overall rotational correlation time $\tau_m = 5$ ns, the correlation time for internal motions $\tau_e = 50$ ps, and the order parameter $S^2 = 0.8$. The angle between the unique axis of the CSA tensor and the internuclear vector r_{IS} is assumed to be $\varphi = 22°$.

The nitrogen is assumed to be relaxed by DD interaction with the proton and by CSA interaction with the external field using $(\sigma_{\parallel} - \sigma_{\perp}) = -160$ ppm.

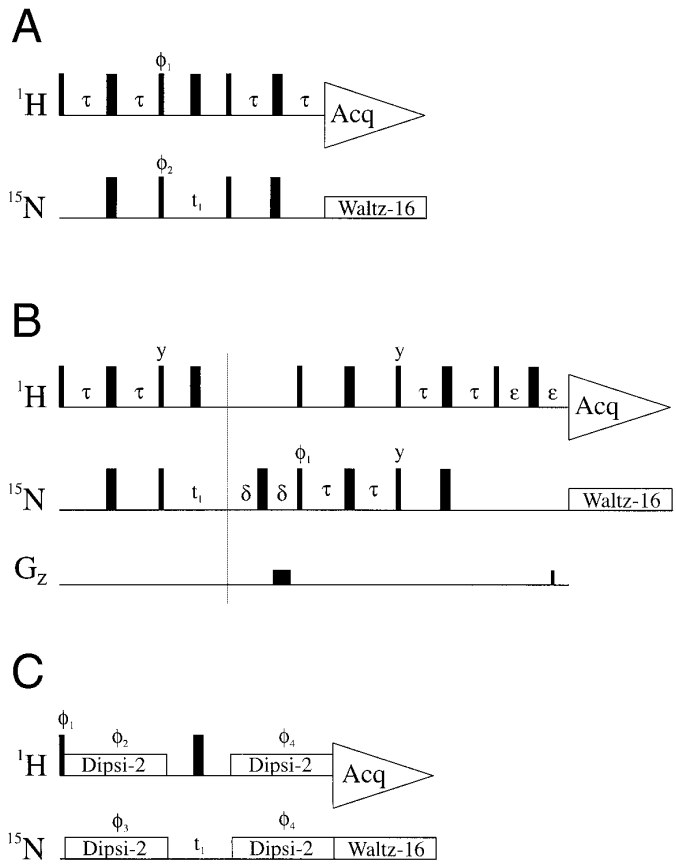

FIG. 1. Pulse sequences for inverse detection ^{1}H–^{15}N correlation experiments for which overall coherence transfer efficiencies are simulated using the developed formalism. Sequence (A) is a phase cycled HSQC experiment (*10*). Sequence (B) is a sensitivity enhanced, phase modulated, gradient selected HSQC experiment (*11*). Sequence (C) is a heteronuclear cross-polarization (CP) based experiment (*12*) with DIPSI-2 (*27*) mixing. All pulse phases are x unless otherwise indicated. Thin and thick vertical bars indicate 90° and 180° pulses, respectively. The ^{15}N RF field strength is 5555 Hz in all pulse sequences. The ^{1}H RF field strength is set to 50,000 Hz for all hard pulses and to 5555 Hz for DIPSI-2 mixing in sequence (C). The time delays are $\tau = \delta = 2.72$ ms and $\epsilon = 0.27$ ms. The pulsed field gradients in sequence (B) are 2.72 and 0.27 ms long and applied with strengths of 30 and ±30.4 G/cm, respectively. The DIPSI-2 mixing times in sequence (C) are 10.36 ms, which corresponds to two (R, $\bar{R}$, $\bar{R}$, R) supercycles. Phase cycling is employed as follows: (A) $\phi 1 = (y, y, -y, -y)$; $\phi 2 = (x, -x, -x, x)$; rec. $= (x, -x)$. (B) $\phi 1 = (x)$; rec. $= (x)$. (C) $\phi 1 = (y, y, -y, -y)$; $\phi 2 = (x, x, -x, -x)$; $\phi 3 = (x, -x, -x, x)$; $\phi 4 = (x, x, -x, -x)$; rec. $= (x, -x, -x, x)$.

The proton experiences DD relaxation due to the nitrogen and a virtual proton at distances of 1.02 and 1.86 Å, respectively. The distance to the virtual proton is calculated by first summing up the distances between each amide proton and all other protons to the power of −6 in a previously determined protein structure (*25*), and then taking this sum to the power of −1/6 (*26*). The average of these amide protons to other protons distances is 1.86 Å. The longitudinal and transverse homonuclear proton DD-relaxation rates,

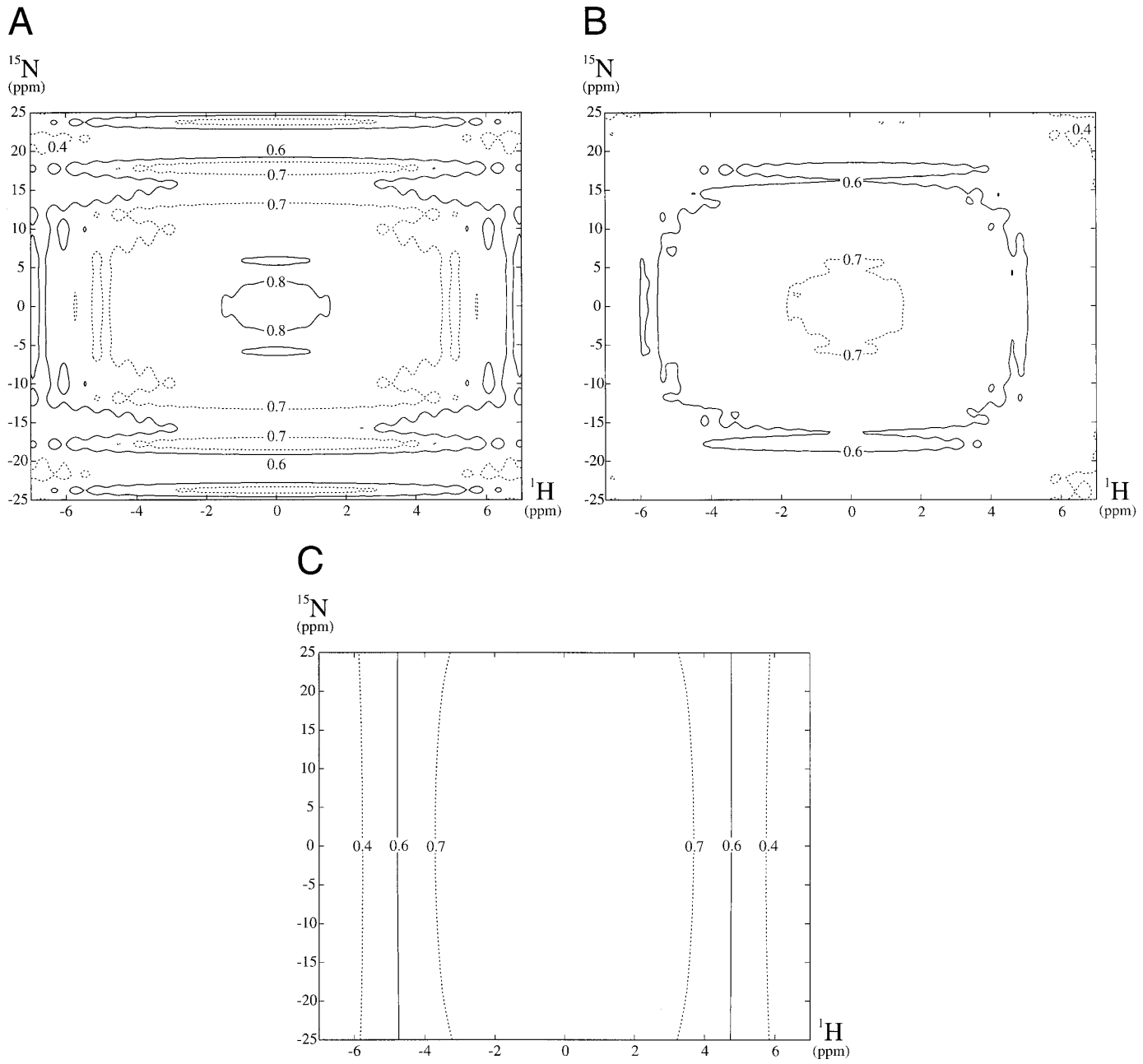

FIG. 2. Simulated transfer efficiencies as a function of offset chemical shifts for (A) a phase cycled HSQC, (B) a sensitivity enhanced HSQC, and (C) a heteronuclear CP based correlation experiment. The remaining fraction of in-phase x or y magnetization at the beginning of the acquisition period is presented as contour levels. The pulse sequences used in the simulations are presented in Fig. 1. The nuclear spins ^{1}H and ^{15}N are coupled together with a scalar coupling constant of 92 Hz. The molecular dynamics important for relaxation are described by the overall rotational correlation time $\tau_m = 5$ ns; the correlation time of internal motions $\tau_e = 50$ ps; and the order parameter $S^2 = 0.8$. Other relevant parameters assumed in the simulations are given in the text.

denoted ρ_H and λ_H, can be calculated using equations similar to Eqs. [24] and [26]:

$$\rho_H = \frac{1}{4}\left(\frac{\mu_0}{4\pi}\right)^2\left(\frac{\hbar\gamma_H^2}{r_{eff}^3}\right)^2[J(0) + 3J(\omega_H) + 6J(2\omega_H)] \quad [39]$$

$$\lambda_H = \frac{1}{8}\left(\frac{\mu_0}{4\pi}\right)^2\left(\frac{\hbar\gamma_H^2}{r_{eff}^3}\right)^2[5J(0) + 9J(\omega_H) + 6J(2\omega_H)]. \quad [40]$$

The static magnetic field strength is set to 14.09 T and the simulations are performed with similar and experimentally real-

istic RF field strengths in order to be able to compare transfer efficiencies. The RF field strength for ^{1}H is 50,000 Hz for all hard pulses. The RF field strength for ^{15}N in all sequences and for ^{1}H DIPSI-2 mixing in sequence (C) is 5555 Hz. The corresponding 90° pulse lengths are 5 and 45 μs, respectively.

Pulse Sequences

The phase cycled HSQC in Fig. 1A (*10*) is implemented as written without any special problems.

The sensitivity enhanced gradient selected HSQC in Fig. 1B (*11*) is more difficult to implement since it includes pulsed field gradients (PFG). We have implemented the PFG in the following way. The effect of a pulsed field gradient is a z rotation identical to the effect of the chemical shift. When the PFG is applied a term proportional to the PFG field strength is added to all chemical shift terms in Eq. [19] according to

$$\Omega_I = \Omega_I - \gamma_I B_0(z)$$
$$\Omega_S = \Omega_S - \gamma_S B_0(z), \qquad [41]$$

where $B_0(z)$ is the strength of the applied PFG as a function of the physical height of the sample tube. Only a single value of z can be used at a time in the numerical calculations, corresponding to a single xy plane in the sample tube. The calculations are therefore repeated with linearly spaced values of z and the normalized results are added. In this way an integration over the height of the sample is performed. When pulsed field gradients are successfully implemented in a pulse sequence the desired magnetizations always have the same phase at the beginning of the acquisition and is added constructively while unwanted magnetizations have random phases and are added destructively. Simulations using different numbers of slices show that 50 planes are sufficient for almost complete cancellation of unwanted magnetization. We have therefore used 50 planes when integrating over the height of the sample, which is assumed to be 1 cm. $B_0(z)$ was assumed to be a linear function of z.

Both echo and antiecho pathways were simulated and subtracted in order to obtain the observable y magnetization in the same way as in real experiments (*11*).

The cross-polarization based experiment in Fig. 1C (*12*) uses simultaneous DIPSI-2 (*27*) mixing on both the ^{1}H and the ^{15}N nuclei. This can easily be simulated using the homogeneous master equation.

Transfer Efficiencies

The transfer efficiencies for the three pulse sequences presented in Figs. 1A–1C are compared in Figs. 2A–2C. The normalized x or y magnetization is presented as a function of offset frequencies in ppm for ^{1}H and ^{15}N. The $t1$ incrementation delay is set to 0.

The ordinary phase cycled HSQC experiment (A) has the highest transferred intensity of the three experiments as well as a large ^{1}H bandwidth. It should be noted that the sensitivity enhanced experiment (B) transfers both x and y magnetization from the ^{15}N dimension to the ^{1}H dimension and is $\sqrt{2}$ more sensitive compared to amplitude modulated experiments for a complete 2D data set. When this effect is taken into account the most efficient experiment is the sensitivity enhanced experiment for the present set of dynamics parameters. The cross-polarization based experiment (C) has the widest ^{15}N and the most narrow ^{1}H bandwidth of all experiments. The transfer surface is also smoother compared to the INEPT based experiments.

DISCUSSION

It is interesting to note that all the common transformation rules of the product operator formalism (*13*) occur as antisymmetrical off-diagonal elements in the matrix of Eq. [19]. The transformations due to chemical shifts, scalar coupling, and RF pulses are clear and these are effective simultaneously, and in competition, with relaxation.

All autorelaxation rates are diagonal elements, whereas the cross-relaxation elements are symmetric off-diagonal elements. It can also be noted that the Bloch equations in the rotating frame (*28*) as well as both the heteronuclear Solomon equations (*29*) and the extended Solomon equations (*9*), are integrated parts of Eq. [19]. The relaxation rates of heteronuclear zero- and double-quantum coherences can be calculated as the difference and sum of the diagonal element λ^{mq} and the off-diagonal element μ^{mq}, respectively.

The spin Hamiltonian for a heteronuclear two-spin system, Eq. [5], includes only one operator, $2I_zS_z$, that can transfer magnetization through the scalar coupling. The average Liouvillian for a complete DIPSI-2 sequence using this Hamiltonian, Eq. [5], can be calculated using Eq. [38]. It contains approximately the planar coupling Hamiltonian, $\pi J(I_yS_y + I_zS_z)$, usually discussed in context of cross-polarization based experiments. The effect of the complicated DIPSI-2 sequence can be simulated with this average Liouvillian. It should be clear that in the doubly rotating frame operator terms such as $2I_xS_x$ and $2I_yS_y$ average to zero rapidly compared to the time scale of a single pulse and cannot be effective for transfer of magnetization. These operator terms should therefore only be included in average Hamiltonians and not in real Hamiltonians.

There are several differences between the theory for heteronuclear spin systems presented here and the theory for homonuclear spin systems presented earlier (*8*). The homonuclear theory includes the strong scalar coupling Hamiltonian which induces rotations not only around $2I_zS_z$, as is the case for heteronuclear theory (see previous paragraph), but also around $2I_xS_x$ and $2I_yS_y$. This makes isotropic mixing

possible for homonuclear spin systems, with twice the rate of transfer compared to cross-polarization for heteronuclear spin systems (*12*). The relaxation terms are calculated differently for homonuclear spin systems, and additional elements appear, including cross-relaxation between transverse magnetization operators (*8*). The use of a doubly rotating frame in the case of the heteronuclear theory prohibits use of the relaxation terms given in our previous formulation of the homonuclear theory.

The method we have used in order to simulate the effect of a pulsed field gradient along the z axis is to the best of our knowledge new. It does not take diffusion into account, but it is in other respects a complete treatment. Shaped pulsed field gradients can easily be implemented using this method. The effect of an inhomogeneous RF field can also be simulated using a similar approach if the inhomogeneity can be described by an axially symmetric function. In this case terms of the form $\omega_x(r, z)$ and $\omega_y(r, z)$ should be used in Eq. [19] and an integration over both the radius and the height of the sample performed.

The average Liouvillian calculated according to Eq. [38] can with advantage be used as a target function in the optimization of, for example, decoupling sequences, mixing sequences, and shaped pulses. It can also be used when developing methods for isolation or decoupling of cross-correlation or cross-relaxation pathways.

CONCLUSIONS

We have presented the complete homogeneous master equation for a heteronuclear two-spin system. The equation is useful in the simulation of heteronuclear pulse sequences when the effect of relaxation cannot be ignored. The homogeneous master equation should also become useful in the development and analysis of pulse sequences in which a specific average relaxation Liouvillian is required. In order to illustrate the applicability of the homogeneous master equation as formulated here, the transfer efficiencies of three heteronuclear pulse sequences, in the presence of relaxation, are calculated.

ACKNOWLEDGMENTS

This work was supported by the Swedish Natural Sciences Research Council, the Magnus Bergwall Foundation, and the Sven and Ebba-Christina Hagbergs Foundation.

REFERENCES

1. A. Abragam, “Principles of Nuclear Magnetism,” Oxford Univ. Press, Oxford (1961).
2. R. R. Ernst, G. Bodenhausen, and A. Wokaun, “Principles of Nuclear Magnetic Resonance in One and Two Dimensions,” Oxford Univ. Press, Oxford (1987).
3. S. A. Smith, T. O. Levante, B. H. Meier, and R. R. Ernst, Computer simulations in magnetic resonance. An object-oriented programming approach, *J. Magn. Reson. A* **106,** 75–105 (1994).
4. J. Jeener, Superoperators in magnetic resonance, *Adv. Magn. Reson.* **10,** 1–51 (1982).
5. S. A. Smith, W. E. Palke, and J. T. Gerig, Superoperator propagators in simulations of NMR spectra, *J. Magn. Reson. A* **106,** 57–64 (1994).
6. M. H. Levitt and L. Di Bari, Steady state in magnetic resonance pulse experiments, *Phys. Rev. Lett.* **69,** 3124–3127 (1992).
7. M. H. Levitt and L. Di Bari, The homogeneous master equation and the manipulation of relaxation networks, *Bull. Magn. Reson.* **16,** 94–114 (1994).
8. P. Allard, M. Helgstrand, and T. Härd, A method for simulation of NOESY, ROESY and off-resonance ROESY spectra, *J. Magn. Reson.* **129,** 19–29 (1997).
9. D. Canet, Construction, evolution and detection of magnetization modes designed for treating longitudinal relaxation of weakly coupled spin $\frac{1}{2}$ systems with magnetic equivalence, *Prog. NMR Spectrosc.* **21,** 237–291 (1989).
10. G. Bodenhausen and D. J. Ruben, Natural abundance nitrogen-15 NMR by enhanced heteronuclear spectroscopy, *Chem. Phys. Lett.* **69,** 185–189 (1980).
11. L. E. Kay, P. Keifer, and T. Saarinen, Pure absorption gradient enhanced heteronuclear single quantum correlation spectroscopy with improved sensitivity. *J. Am. Chem. Soc.* **114,** 10663–10665 (1992).
12. M. Ernst, C. Griesinger, R. R. Ernst, and W. Bermel, Optimized heteronuclear cross polarization in liquids, *Mol. Phys.* **74,** 219–252 (1991).
13. O. W. Sørensen, G. W. Eich, M. H. Levitt, G. Bodenhausen, and R. R. Ernst, Product operator formalism for the description of NMR pulse experiments, *Prog. NMR Spectrosc.* **16,** 163–192 (1983).
14. C. N. Banwell and H. Primas, On the analysis of high-resolution nuclear magnetic resonance spectra I. Methods of calculating NMR spectra, *Mol. Phys.* **6,** 225–256 (1963).
15. M. Guéron, J. L. Leroy, and R. H. Griffey, Proton nuclear magnetic relaxation of ^{15}N-labeled nucleic acids via dipolar coupling and chemical shift anisotropy, *J. Am. Chem. Soc.* **105,** 7262–7266 (1983).
16. M. Goldman, Interference effects in the relaxation of a pair of unlike spin-$\frac{1}{2}$ nuclei, *J. Magn. Reson.* **60,** 437–452 (1984).
17. A. G. Redfield, The theory of relaxation processes, *Adv. Magn. Reson.* **1,** 1–32 (1965).
18. H. Desvaux, P. Berthault, N. Birlirakis, and M. Goldman, Off-resonance ROESY for the study of dynamic processes, *J. Magn. Reson. A* **108,** 219–229 (1994).
19. J. Cavanagh, W. J. Fairbrother, A. G. Palmer III, and N. J. Skelton, “Protein NMR Spectroscopy: Principles and Practice,” Academic Press, San Diego (1996).
20. J. W. Peng and G. Wagner, Mapping of spectral density functions using heteronuclear NMR relaxation measurements, *J. Magn. Reson.* **98,** 308–332 (1992).
21. J. W. Peng and G. Wagner, Protein mobility from multiple ^{15}N relaxation parameters, *in* “Understanding Chemical Reactivity” (R. Tycko, Ed.), pp. 373–454, Kluwer Academic Publishers, Dordrecht (1994).
22. G. Lipari and A. Szabo, Model-free approach to the interpretation of nuclear magnetic resonance relaxation in macromolecules. 1.

Theory and range of validity, *J. Am. Chem. Soc.* **104,** 4546–4559 (1982).

23. G. Lipari and A. Szabo, Model-free approach to the interpretation of nuclear magnetic resonance relaxation in macromolecules. 2. Analysis of experimental results, *J. Am. Chem. Soc.* **104,** 4559–4570 (1982).

24. N. Tjandra, A. Szabo, and A. Bax, Protein backbone dynamics and ^{15}N chemical shift anisotropy from quantitative measurement of relaxation interference effects, *J. Am. Chem. Soc.* **118,** 6986–6991 (1996).

25. H. Baumann, S. Knapp, T. Lundbäck, R. Ladenstein, and T. Härd, Solution structure and DNA-binding properties of a thermostable protein from the archeon *Sulfolobus solfataricus, Nature Struct. Biol.* **1,** 808–819 (1994).

26. P. Allard, J. Jarvet, A. Ehrenberg, and A. Gräslund, Mapping of the spectral density function of a C^{α}–H^{α} bond vector from NMR relaxation rates of a ^{13}C-labelled α-carbon in motilin, *J. Biomol. NMR* **5,** 133–146 (1995).

27. A. J. Shaka, C. J. Lee, and A. Pines, Iterative schemes for bilinear operators; application to spin decoupling, *J. Magn. Reson.* **77,** 274–293 (1988).

28. F. Bloch, Nuclear induction, *Phys. Rev.* **70,** 460–474 (1946).

29. I. Solomon, Relaxation processes in a system of two spins, *Phys. Rev.* **99,** 559–565 (1955).